THE INFLUENCE OF SECOND PHASE INCLUSIONS ON DYNAMIC FRACTURE OF TWO-PHASE ALLOYS

S. PYTEL, L. WOJNAR, H. KIEŁKUCKI [x]

Tensile tests were carried out on flat, one-side polished and cylindrical specimens which were deformed at the following strain rates: $\dot{\varepsilon} = 2 \cdot 10^{-3}$, $3 \cdot 10^{2}$, 10^{3} (s^{-1}). Four, two-phase alloys, based on ferritic matrix with nodular graphite, silicates and sulphides and eutectic sulphides were examined. Introduced void growth ratio ϑ allowed the strain rate effect to be estimated and the void growth process to be characterized during dynamic fracture.

INTRODUCTION

Second phase inclusions have important effects on strength and toughness of two- phase alloys. The presence of the second phase particles can cause major changes in ductility and, although mechanistic effects are well established, the quantitative relationship between ductility and microstructure is still elusive, especially for dynamic fracture. In this report, an attempt to describe quantitatively the effect of second phase inclusions on dynamic toughness of selected two-phase alloys was undertaken.

Numerous studies of two- phase alloys composed of a ductile matrix with hard, second-phase inclusions showed that during deformation one can differentiate a few characteristic stages after Rogers (1) and Broek (2), namely:
I - nucleation of microcracks which is a process of crack appearance inside a particle, or void nucleation at the particle-matrix boundary,
II - local void growth without matrix failure,
III - microcrack coalescence as a result of the loss of matrix continuity leading to the failure of a specimen.

As was shown in previous papers by Pytel and Rudnik (3) and Pytel and Wojnar (4) for non-metallic inclusions of compact shape, the prevailing nucleation mechanism is void formation at the particle-matrix boundary; the low strength of this boundary surface is the most probable reason for this phenomenon.

[x] Institute of Material Science, Cracow Technical University, ul. Warszawska 24, 31-155 Cracow, POLAND.

Assuming the existance of plane strain one can describe the void growth ratio, defined after Pytel and Rudnik (3) as follows:

$$\vartheta = \frac{d\bar{\varepsilon}}{d\bar{\varphi}} \tag{1}$$

for a collection of particles. In several references, for example Gurland and Plateau (5), Bellot and Gantois (6), one can find functions describing the ratio ϑ. These functions after being put into relation 1 and further integration gives the void growth relationship as

$$\bar{\varepsilon} = F(\bar{\varphi}) \tag{2}$$

In this paper we assume $\vartheta = k = \text{const.}$ and then:

$$\bar{\varepsilon} = k(\bar{\varphi} - \varphi_n) \tag{3}$$

because $\varphi_n \approx 0$, finally

$$\bar{\varepsilon} = k\bar{\varphi} \tag{4}$$

EXPERIMENTAL PROCEDURE

Materials

Three low-carbon steels designated in paper by A, B and D and one cast iron C were used as materials for investigation. Their chemical composition is given in Table 1. Materials A, B and C have been investigated in the as-cast condition while material D has been hot rolled at 1100 - 1200 K. All materials had a two-phase structure composed of a ferritic matrix with trace quantities of pearlite and second-phase inclusions which were identified as follows:
material A - globular MnS (type I),
material B - eutectic MnS (type II),
material C - nodular graphite,
material D - globular (Fe, Mn)-silicates.

Microscopic observations showed that the type I sulphides, nodular graphite and silicates were randomly dispersed in the ferritic matrix while most of the type II sulphides appeared at the grain boundaries.

In addition, some measurements of stereological parameters were done. These results are given in Table 2.

Table 1. Chemical composition

Material		A	B	C	D
C	%	0.09	0.10	3.60	0.11
Si	%	0.05	0.05	2.80	0.35
Mn	%	1.50	1.14	0.10	0.34
S	%	0.105	0.310	0.013	0.016
P	%	0.015	0.063	0.080	0.020

Table 2. Stereological parameters of inclusions

Material		A	B	C	D
N_A	mm^{-1}	21.8	58.0	86.2	13.8
V_V	%	0.32	0.87	11.2	0.26
$\bar{d}$	μm	8.9	4.3	45.3	24.5

Specimens and testing procedure

Cylindrical and flat, one-side polished, specimens having the dimensions shown in fig.1 were used. Cylindrical specimens were pulled in groups of five at three strain rates, namely $\dot{\varphi}_1 = 2 \cdot 10^{-3}$, $\dot{\varphi}_2 = 3 \cdot 10^{2}$ and $\dot{\varphi}_3 = 10^{3}\ (s^{-1})$. The tests were carried out with the use of tensile test machine, drop weight hammer and explosive tensile device designed by Kiełkucki (7).

Flat specimens underwent tensile tests at the same strain rate ranges. Static tests were carried out using auxiliary equipment (for tensile testing with simultaneous microscopic observation) mounted on the table of a metallographic microscope - Pytel and Rudnik (3).

Results

On the basis of diameter measurements in the necking zone of the specimens, the true strain distribution φ_x versus the distance from the fracture surface x was established. Assuming incompressibility of the material one obtains:

$$\varphi_x = 2 \ln \frac{D_o}{D_x} \tag{5}$$

Results of these investigations are shown in fig.2.

During static tensile tests of flat specimens, load-displacement curves were recorded. Moreover the increase in the average void size was measured and the ratio ϑ for 30 randomly chosen inclusions was calculated. These results are presented in fig.3. In the case of dynamically loaded flat specimens measurements of void sizes were carried out only after rupture (there was no possibility of a continuous measurement). Ratio ϑ was estimated on the basis of these measurements.

Table 3. Value of ratio ϑ for statically and dynamically loaded flat specimens

Material			A	B	C	D
$\dot{\varphi}$	s^{-1}	$2 \cdot 10^{-3}$	2.7±0.63	5.5±1.32	1.9±0.38	2.1±0.23
		10^{3}	3.6±0.82	6.0±1.48	2.3±0.58	3.0±0.37

In order to compare structural phenomena in the vicinity of various inclusions, all tested specimens were carefully examined with the use of SEM type JSM 50, some examples of elongated and coalesced voids are given in fig.4.

DISCUSSION

According to the relationships shown in fig.2, it is note that materials A, C and D have similar strain distributions in the necking zone. Material B with type II sulphides has significantly lower elongation in the neck region. Independent of the relations mentioned above, the diagrams show the decrease of elongation with increasing strain rate for all the materials.

Detailed microscopic observations showed that during static tests, void nucleation began at a strain of about $\bar{\varphi} = 0.0015 - 0.05$ (earlier for larger particles). This means that for all the types of particles examined, the interface boundary is weak enough to form discontinuities at the beginning of plastic flow (as shown for example in fig.4a, b).

Quantitative investigations of the void growth for type I sulphides, silicates and nodular graphite revealed that the difference between their void growth ratios are significantly lower in comparison with the same ratio for material B (see Table 3). Moreover, only in material B, was the phenomenon of void coalescence by shear fracture (fig.4c) or matrix rupture (fig.4d) between particles observed. This effect was already visible during stable elongation of the specimen. It is probably connected with the short inter-inclusion distance (comparable to the inclusion diameter) and also the cylindrical of eutectic sulphides. In consequence, the macroscopic toughness of material B is much lower than the others.

All the materials tested are characterized by an increasing ratio $\bar{v}$ during dynamic loading, especially in materials A and D. In other words, the increase of strain rate causes more intensive void growth. Therefore, the material attains conditions necessary for void coalescence at lower strain with smaller necking of the specimen. This is supported by the experimental observations (see fig.2). Taking into consideration the experimental procedure which is based on surface measurements, these results cannot be fully applicable for describing internal-structure phenomena in cylindrical specimens.

This short report is only an attempt to explain the complex phenomena of ductile fracture of metals, especially during dynamic loading. Further researches including stereology and the nature of second-phase particles are necessary.

CONCLUSIONS

The ratio of void growth $\bar{v}$ is a quantitative criterion characterizing the void growth process during ductile fracture of alloys composed of matrix and second-phase inclusions. A change of strain rate from $2 \cdot 10^{-3}$ (s^{-1}) to 10^{3} (s^{-1}) causes an increase of the ratio $\bar{v}$.

LIST OF SYMBOLS

D_o = original specimen diameter (mm)

D_x = specimen diameter after fracture at a distance x from fracture surface (mm)

$\bar{d}$ = mean particle diameter (um)

$d\bar{\varepsilon}$, $d\bar{\varphi}$ = elementary increase of $\bar{\varepsilon}$ and $\bar{\varphi}$

F = function, relationship

k = constant value

N_A = number of particles per unit test area (mm^{-2})

V_V = volume fraction (%)

x = distance from crack surface (mm)

$\bar{\varepsilon}$ = mean true strain of void

$\bar{\varphi}$ = mean true strain of specimen

φ_n = as above, at the moment of first void nucleation

φ_x = true strain of specimen at a distance x from crack surface

$\dot{\varphi}$ = strain rate (s^{-1})

σ = tensile stress (MPa)

$\bar{v}$ = mean void growth ratio

REFERENCES

1. Rogers, H., Trans. AIME, 218 1960 498.
2. Broek, D., Eng. Fract. Mech., 5 1973 55.
3. Pytel, S., and Rudnik, S., Archiw. Hutn., 24 1979 58.
4. Pytel, S., and Wojnar, L., Proc. 11th Conf. on Phys. Met., Częstochowa, Poland 1983 81.
5. Gurland, J., and Plateau, J., Trans. ASM, 56 1963 442.
6. Bellot, J., and Gantois, M., Trans. ISI, 18 1978 546.
7. Kiełkucki, H., "The explosive tensile device", not published.

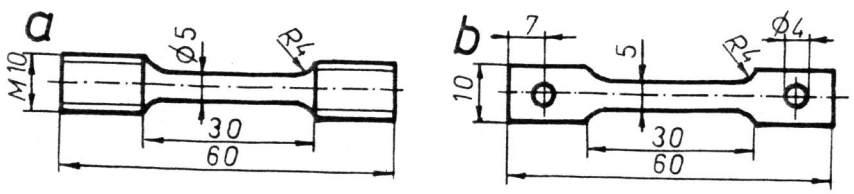

Fig.1 Cylindrical (a) and flat (b) specimens for tensile tests.

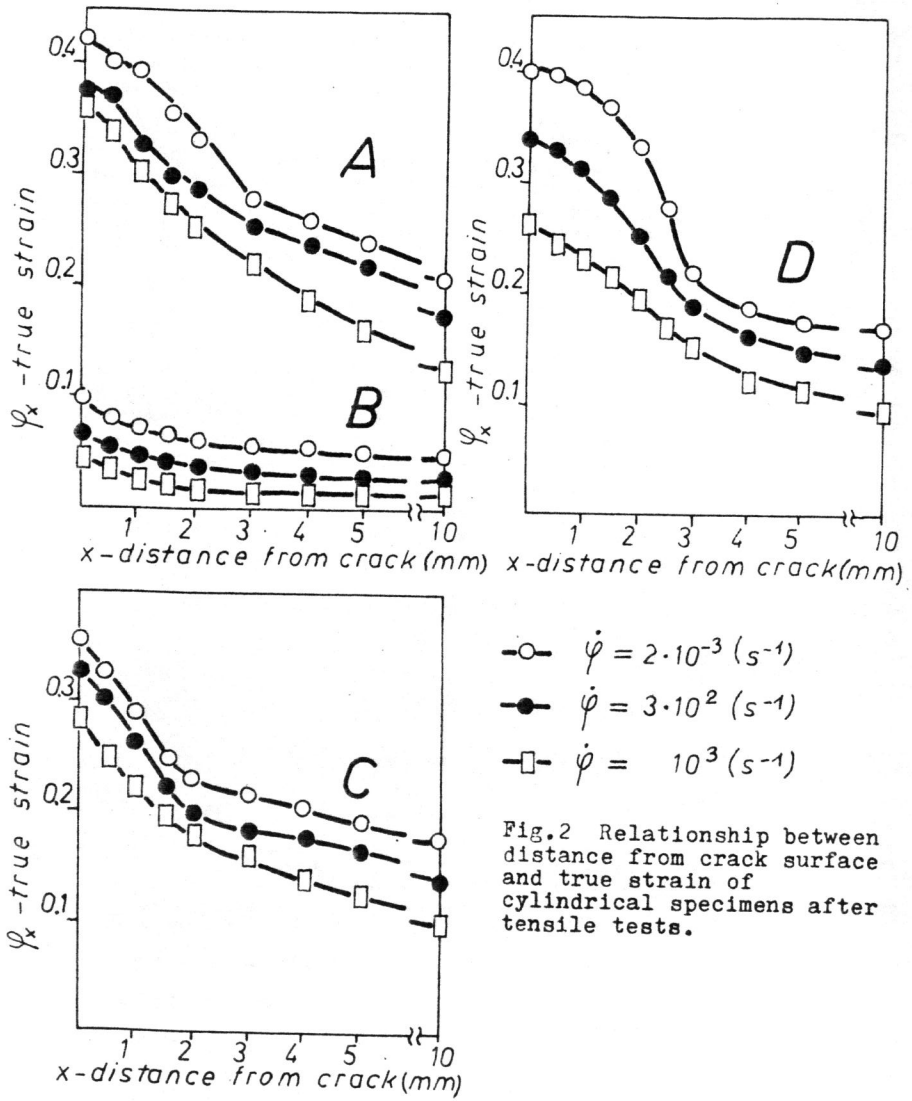

Fig.2 Relationship between distance from crack surface and true strain of cylindrical specimens after tensile tests.

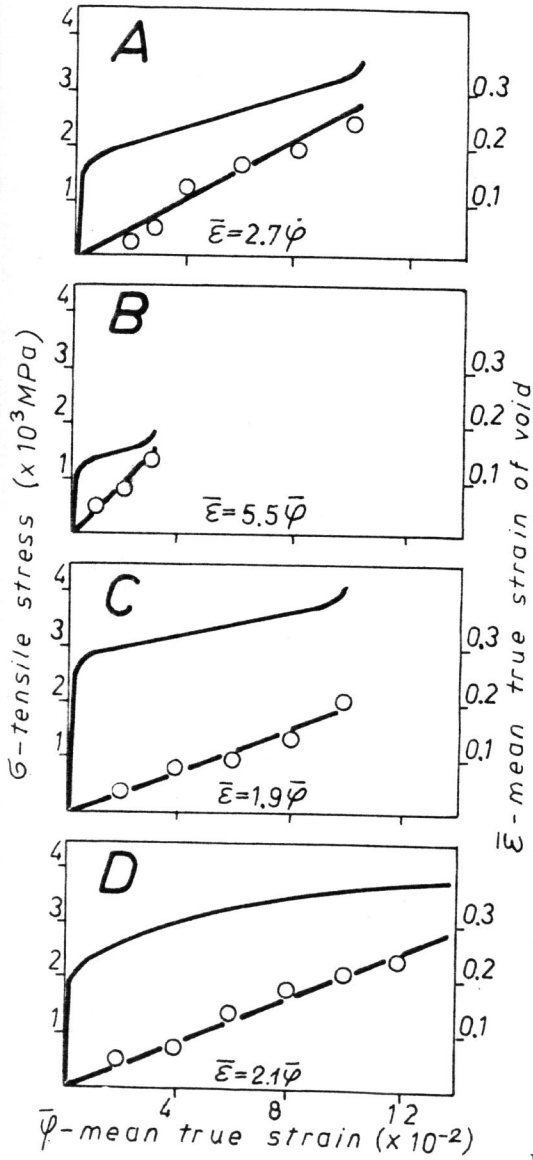

Fig.3 Tensile stress and void true strain versus specimen true strain.

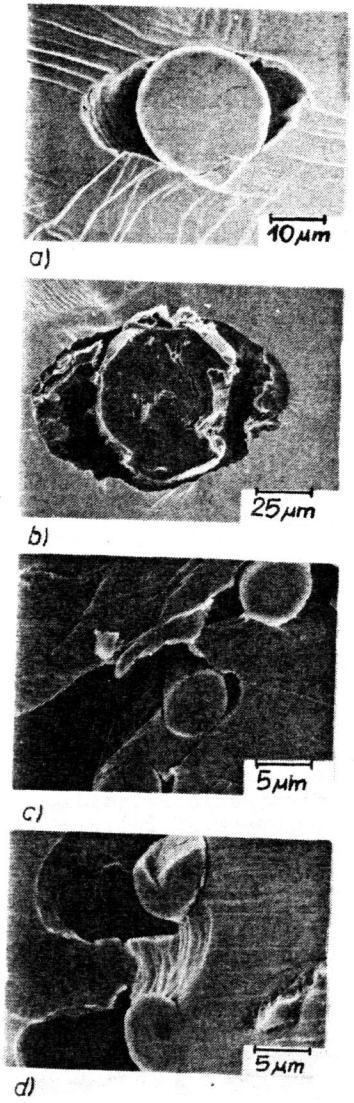

Fig.4 Void growth in vicinity of particles: a-sulphide type I, b-graphite. Coalescence of voids for sulphides type II: c-shear fracture d-rupture of matrix.